PAGEOPH, Vol. 142, No. 3/4 (1994)

0033–4553/94/040467–23$1.50 + 0.20/0

Some Comparisons between Mining-induced and Laboratory Earthquakes

A. McGARR[1]

Abstract—Although laboratory stick-slip friction experiments have long been regarded as analogs to natural crustal earthquakes, the potential use of laboratory results for understanding the earthquake source mechanism has not been fully exploited because of essential difficulties in relating seismographic data to measurements made in the controlled laboratory environment. Mining-induced earthquakes, however, provide a means of calibrating the seismic data in terms of laboratory results because, in contrast to natural earthquakes, the causative forces as well as the hypocentral conditions are known. A comparison of stick-slip friction events in a large granite sample with mining-induced earthquakes in South Africa and Canada indicates both similarities and differences between the two phenomena. The physics of unstable fault slip appears to be largely the same for both types of events. For example, both laboratory and mining-induced earthquakes have very low seismic efficiencies $\eta = \tau_a/\bar{\tau}$, where τ_a is the apparent stress and $\bar{\tau}$ is the average stress acting on the fault plane to cause slip; nearly all of the energy released by faulting is consumed in overcoming friction. In more detail, the mining-induced earthquakes differ from the laboratory events in the behavior of η as a function of seismic moment M_0. Whereas for the laboratory events $\eta \simeq 0.06$ independent of M_0, η depends quite strongly on M_0 for each set of induced earthquakes, with 0.06 serving, apparently, as an upper bound. It seems most likely that this observed scaling difference is due to variations in slip distribution over the fault plane. In the laboratory, a stick-slip event entails homogeneous slip over a fault of fixed area. For each set of induced earthquakes, the fault area appears to be approximately fixed but the slip is inhomogeneous due presumably to barriers (zones of no slip) distributed over the fault plane; at constant $\bar{\tau}$, larger events correspond to larger τ_a as a consequence of fewer barriers to slip. If the inequality $\tau_a/\bar{\tau} \leq 0.06$ has general validity, then measurements of $\tau_a = \mu E_a/M_0$, where μ is the modulus of rigidity and E_a is the seismically-radiated energy, can be used to infer the absolute level of deviatoric stress at the hypocenter.

Key words: Stick-slip friction, mining-induced earthquakes, seismic efficiency.

Introduction

Since the suggestion by BRACE and BYERLEE (1966) that stick-slip friction in the laboratory is analogous to natural crustal earthquakes, there has been substantial progress in understanding each of these phenomena (e.g., SCHOLZ, 1990) and the laboratory results have been used as a basis for models of earthquake genesis

[1] U.S. Geological Survey, MS977, 345 Middlefield Rd., Menlo Park, CA 94025-3591, U.S.A.

(e.g., DIETERICH, 1992). For the most part, however, progress in these two fields, laboratory friction and earthquake seismology, has proceeded along separate paths. In particular, seismologists rarely relate their measures of the earthquake source to corresponding laboratory results. There are good reasons for such oversights. First, the comparison of earthquake source parameters to their counterparts in laboratory experiments is difficult because, in contrast to the well-controlled laboratory environment, the earthquake source is generally inaccessible and anything but controlled, thus rendering many of its measures quite model dependent. Second, in contrast to laboratory samples, the applied forces responsible for earthquakes are unknown.

Mining-induced earthquakes offer a means of narrowing the conceptual gap between laboratory friction experiments and seismological measures of earthquake sources inasmuch as, in contrast to natural earthquakes, the forces that give rise to mine tremors are at least moderately understood and the source region is often accessible to direct observation (e.g., COOK, 1963; ORTLEPP, 1978; GAY and ORTLEPP, 1979; MCGARR *et al.*, 1979). Hence, some meaningful comparisons between the two types of events are feasible. To demonstrate that such comparisons can provide useful insights regarding earthquake source processes, I review here some results from both the laboratory and hard-rock mines that are especially amenable to comparison.

Figure 1 illustrates some of the issues to be explored here. A fault of area A is loaded to failure by an applied shear stress τ_1. During the seismic event, slip increases to its final value D as the loading stress decreases from τ_1 to its final value τ_2; the slope of the line representing the reduction in loading stress is the unloading stiffness of the system. At the same time, the frictional resisting stress drops abruptly from its initial value τ_1 to a lower average value $\bar{\tau}_r$ between τ_1 and τ_2.

The energy W released by the slip event is

$$W = \left(\frac{\tau_1 + \tau_2}{2}\right) DA = \bar{\tau} DA \tag{1}$$

where $\bar{\tau} = (\tau_1 + \tau_2)/2$. The energy dissipated in overcoming friction E_r is given by

$$E_r = \bar{\tau}_r DA. \tag{2}$$

By definition, the apparent stress τ_a is the difference between the average loading and the average resisting stress (e.g., SAVAGE and WOOD, 1971). Thus,

$$\tau_a = \bar{\tau} - \bar{\tau}_r \tag{3}$$

and the radiated seismic energy E_a is

$$E_a = \tau_a AD. \tag{4}$$

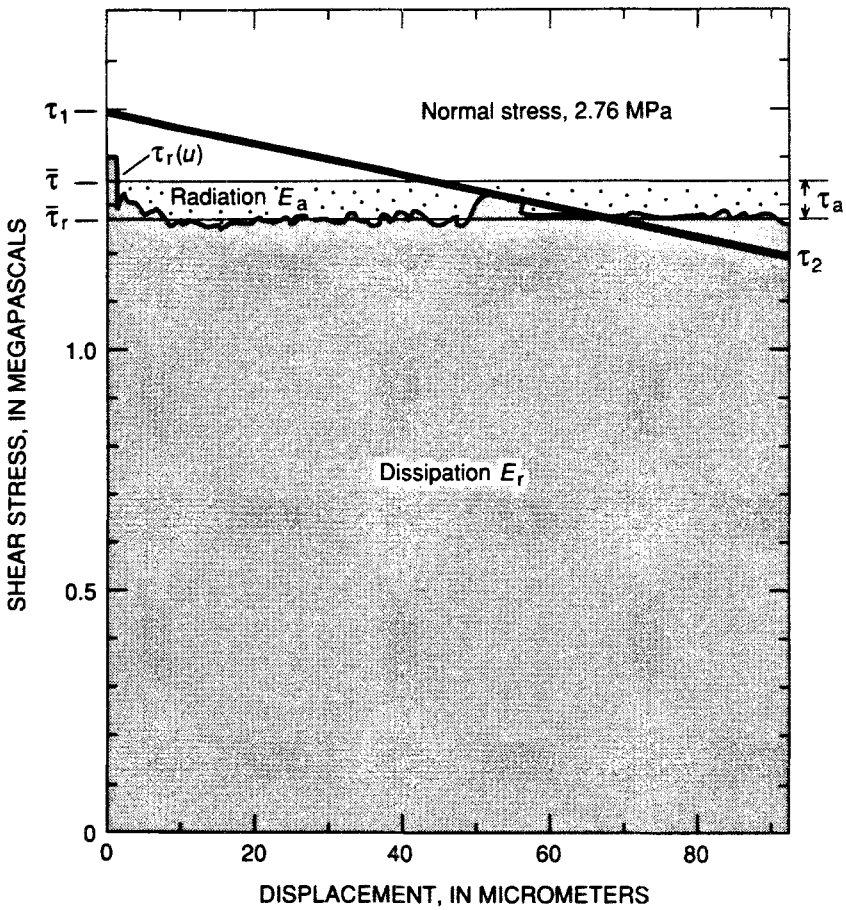

Figure 1
Relation between resisting stress and displacement in an unloading elastic medium (inclined line with slope -3.3 MPa/mm) during an earthquake. As slip increases, stress in the rock diminishes linearly from τ_1 to τ_2, with average value $\bar{\tau}$. The area under this line is the total work expended per unit fault area; the area below the curve of resisting stress τ_r is the energy dissipated per unit fault area. The difference between the total work expended and the dissipated energy (shaded area) is the work done by the apparent stress τ_a (stippled area) that is available for seismic ground motion. (Adapted from Figure 10.3 of LACHENBRUCH and MCGARR (1990) and based on a laboratory experiment on a large granite sample reported by LOCKNER and OKUBO (1983).)

Accordingly, the seismic efficiency η, which is the fraction of released energy radiated seismically is

$$\eta = E_a/W = \tau_a/\bar{\tau}. \tag{5}$$

Finally, the stress drop $\Delta\tau$ is simply

$$\Delta\tau = \tau_1 - \tau_2. \tag{6}$$

Because the seismic moment M_0 is defined as

$$M_0 = \mu AD \tag{7}$$

where μ is the modulus of rigidity, an alternative to (3) used by seismologists for estimating the apparent stress is (e.g., WYSS and BRUNE, 1968)

$$\tau_a = \frac{\mu E_a}{M_0}. \tag{8}$$

Similarly the alternative to (6) most commonly used (KEILIS-BOROK, 1959) for calculating earthquake stress drop is

$$\Delta\tau = \frac{7}{16} M_0 / r_0^3 \tag{9}$$

where the earthquake source is modeled as slip across a penny-shaped crack of radius r_0 given by (BRUNE, 1970)

$$r_0 = \frac{2.34\beta}{2\pi f_0} \tag{10}$$

where the corner frequency f_0 is essentially the inverse of the source duration.

A number of issues of importance to seismologists are represented in Figure 1. First is the question of how earthquakes scale. That is, do τ_a and $\Delta\tau$ vary with earthquake size M_0? Second, the efficiency η of earthquakes has been debated at length without any resolution (e.g., LACHENBRUCH and MCGARR, 1990). Third, can the seismic radiation of an earthquake reveal anything about the absolute state of deviatoric stress causing the event (e.g., SCHOLZ, 1990; MCGARR, 1984)?

For laboratory stick-slip events, these questions are readily resolved by direct measurement. Thus, the central question addressed here involves the extrapolation of laboratory results for purposes of answering these same questions for earthquakes. LOCKNER and OKUBO (1983) reported stick-slip friction results that are especially useful for exploring the issues just mentioned. In particular, the laboratory set-up (DIETERICH, 1979, 1981) used by those authors includes not only the capability of monitoring the loading stress and the fault slip, but, more uniquely, yields measurements of the resisting stress.

The induced earthquake data sets reviewed here, for comparison with the laboratory events, were recorded in South Africa and Canada. The tremors receiving the most emphasis occurred in two gold mining districts of South Africa (MCGARR *et al.*, 1989) during some special experiments involving broad-band wide-dynamic range underground recording (MCGARR, 1992a,b, 1993) between 1986 and 1989. This data set is well suited to investigating the issues of interest here because the exceptionally-clear waveforms indicate not only the slip across faults in the rock abutting ore production, but, also, in many cases, the coseismic volume reduction of the nearby stopes (MCGARR, 1992a); measurement of this volume

reduction yields the coseismic energy release (e.g., COOK, 1963; COOK *et al.*, 1965; MCGARR, 1976) and, thereby, the average stress acting to cause fault slip.

Induced earthquakes due to shaft excavation at depths near 400 m in the Underground Research Laboratory (URL), Manitoba, Canada, are quite useful for the present analysis because they occurred in a well-controlled environment in which both apparent stresses (GIBOWICZ *et al.*, 1991) and the state of stress (MARTIN and YOUNG, 1993) have been measured. Interestingly, most of these events are smaller than the laboratory events, as will be seen.

Mining-induced tremors in the Strathcona mine, near Sudbury, Canada, are of interest here in that apparent stresses reported by URBANCIC and YOUNG (1993) can be compared quite directly to both the URL and the laboratory stresses inasmuch as the magnitude ranges of these three data sets overlap. As for the URL events, these small Strathcona earthquakes were recorded with very broad bandwidth and wide dynamic range (e.g., YOUNG *et al.*, 1989), and at small hypocentral distances, thus, rendering both of these Canadian data sets exceptionally free of unwanted artifacts.

Generally, then, this study involves primarily the comparison between laboratory stick-slip events and three sets of mining-induced earthquakes in terms of various seismic source parameters with the intention of calibrating the earthquake parameters. Additionally, some earthquake results are considered here primarily to indicate the plausibility of scaling upward from the small magnitude induced and laboratory events to the realm of major crustal earthquakes. Of particular interest, these observations provide an opportunity to pursue the proposal by SCHOLZ (1990, p. 91) that the seismic stress changes (Figure 1) are related systematically to the total shear stress acting on the fault.

Laboratory Earthquakes

Energy budgets of stick-slip events in large biaxially-loaded samples (DIETERICH, 1981) were reported by LOCKNER and OKUBO (1983) in a format especially conducive to comparison with earthquakes. The granite sample, $1.5 \times 1.5 \times 0.4\ m^3$, with a diagonal saw cut, is loaded by means of inflating flat jacks at the edges. In this way, both the shear stress τ and the normal stress σ_n, loading the precut fault of area $2 \times 0.4\ m^2$, can be controlled. In the stick-slip experiments, the time histories of resisting stress τ_r and particle velocity are monitored using strain gauges and velocity transducers, respectively. Fault slip is measured using either velocity or displacement transducers.

Table 1, derived from information presented by LOCKNER and OKUBO (1983), lists various measures of the stick-slip process. In these experiments, the stress drop $\Delta\tau$ is related to the fault slip according to the unloading stiffness S of 3.3 MPa/mm (Figure 1). After estimating the apparent stress using (3) the efficiency is obtained

Table 1

Laboratory stick-slip friction data. (Adapted from Table 1 of LOCKNER and OKUBO, 1983)

Event*	σ_n MPa	τ_1 MPa	D μm	$\Delta\tau$ MPa	$\bar{\tau}$ MPa	$\bar{\tau}_r$ MPa	τ_a MPa	$\eta = \tau_a/\bar{\tau}$	$\Delta\tau/\bar{\tau}$	M_0 N-m	M
5	1.66	0.94	62	0.20	0.84	0.80	0.04	0.048	0.24	1.24×10^6	−1.94
6	1.66	0.98	70	0.23	0.86	0.85	0.01	0.012	0.27	1.40×10^6	−1.90
7	2.21	1.21	73	0.24	1.09	1.03	0.06	0.055	0.22	1.46×10^6	−1.89
8	2.21	1.26	84	0.28	1.12	1.07	0.05	0.045	0.25	1.68×10^6	−1.85
9	2.76	1.49	93	0.31	1.34	1.26	0.08	0.060	0.23	1.86×10^6	−1.82
10	2.76	1.53	97	0.32	1.37	1.30	0.07	0.051	0.23	1.94×10^6	−1.81
11	3.31	1.83	145	0.48	1.59	1.52	0.07	0.044	0.30	2.90×10^6	−1.69
12	3.31	1.83	128	0.42	1.62	1.52	0.10	0.062	0.26	2.56×10^6	−1.73
13	4.41	2.34	127	0.42	2.13	1.96	0.17	0.080	0.20	2.54×10^6	−1.73
14	4.41	2.40	142	0.47	2.17	2.02	0.15	0.069	0.22	2.84×10^6	−1.70
15	4.41	2.21	119	0.39	2.02	1.93	0.09	0.045	0.19	2.38×10^6	−1.75
16	4.41	2.27	134	0.44	2.05	1.96	0.09	0.044	0.21	2.68×10^6	−1.71
17	4.41	2.07	74	0.24	1.95	1.84	0.11	0.056	0.12	1.48×10^6	−1.89
18	4.41	2.20	105	0.35	2.03	1.91	0.12	0.059	0.17	2.10×10^6	−1.79
19	3.45	1.98	126	0.42	1.77	1.70	0.07	0.040	0.24	2.52×10^6	−1.73

* All experiments were on dry samples.

from (5) and, as noted by LOCKNER and OKUBO (1983), η generally falls in the range of 0.04 to 0.08. Thus, for these stick-slip events, most of the energy released during seismic slip is consumed in overcoming frictional resistance and manifests itself as heat.

Seismic moments for the stick-slip events (Table 1) were calculated using (7) with $A = 0.8$ m^2 and $\mu = 2.5 \times 10^4$ MPa (LOCKNER and OKUBO, 1983). The largest event, number 11, exceeds the smallest, number 5, by a factor of 2.3. From these moments, moment magnitudes M are computed from (HANKS and KANAMORI, 1979)

$$M = (\log M_0 - 9)/1.5 \tag{11}$$

which range from −1.94 to −1.69.

Note that in several respects the moment and magnitude assignments in Table 1 may not be entirely appropriate. First, the laboratory earthquake entails deformation of the loading system as well as slip across the granite sample; (7), of course, does not take this deformation exterior to the sample into account. Second, the stiffness of the total system, which includes the frame, flat jacks and sample (DIETERICH, 1981) is substantially less than that of a crack of equivalent area within granite (e.g., WALSH, 1971); thus, using the modulus of rigidity μ for the granite may not be strictly correct. As will be seen, however, these potential deficiencies in the moment assignments are not likely to matter much in the comparisons emphasized here.

Overshoot

As seen in Figure 1, the loading stress diminishes from τ_1 to τ_2, which is less than the average frictional resisting stress. If the slip is arrested by friction and if τ_r does not vary much from its average dynamic value during the stick-slip event then τ_2 must be less than $\bar{\tau}_r$ (e.g., SAVAGE and WOOD, 1971). If the coefficient of friction displays more exotic behavior, for example, dropping to a very low value after the initiation of slip but then increasing substantially near the end of the event (e.g., BRUNE, 1976; HEATON, 1990) then undershoot is possible; that is $\tau_1 > \tau_2 > \bar{\tau}_r$. To date, however, such behavior has not been reliably observed in laboratory stick-slip friction experiments. Instead overshoot (Figure 1) is observed; the few exceptions to this rule are probably attributable to experimental error.

The amount of overshoot can be calculated from the ratio $\tau_a/\Delta\tau$ (Table 1). If, during the seismic event the loading stress diminished exactly to $\bar{\tau}_r$ then, by definition there is no overshoot: $\bar{\tau} = (\tau_1 + \bar{\tau}_r)/2$ so that $\tau_a = 0.5\,\Delta\tau$ (Figure 1). For 100 percent overshoot, $\bar{\tau}$ coincides with $\bar{\tau}_r$, which implies $\tau_a = 0$ (no seismic radiation). Thus, generally, $0 \leq \tau_a/\Delta\tau \leq 0.5$ (SAVAGE and WOOD, 1971), unless τ_r displays behavior distinctly different from that seen in Figure 1. The observed ratio (Table 1) falls in the range $0.04 \leq \tau_a/\Delta\tau \leq 0.45$ with a median value of 0.23. Interestingly, these laboratory data also do not provide support for the "Orowan condition" of neither undershoot nor overshoot ($\tau_a/\Delta\tau = 0.5$) (e.g., VASSILIOU and KANAMORI, 1982; HOUSTON, 1990).

South African Mine Tremors

Mining-induced earthquakes in the deep gold mines of the Witwatersrand have been of substantial interest for understanding the seismic source, because, in contrast to natural earthquakes, the source of energy for these events is known. Essentially, the gravitational collapse of mine stopes releases energy that is associated with induced earthquakes. Comparisons between the total radiated seismic energy of suites of events with the calculated gravitational energy release over the same period of time (e.g., COOK, 1963; COOK *et al.*, 1965; MCGARR, 1976) indicated low estimates of seismic efficiency of the order of 0.01, or less. A loophole in this argument, however, was the possibility that the primary deformational response of the abutting rock is aseismic creep instead of seismic failure.

This loophole was recently closed, however, in the following way. The clear waveforms of tremors recorded at small hypocentral distance, either underground or at surface stations on hard rock with no site resonances in the frequency band of interest, are so rich in source information that complete moment tensor solutions can be determined with little uncertainty (MCGARR, 1992a). The resulting moment

tensors can then be decomposed into volumetric and deviatoric components (McGARR, 1992a,b) as will be reviewed. These coseismic volume reductions, in turn, indicate the energy release W, which can be compared to the radiated seismic energy E_a and it turns out that the seismic efficiency is, indeed, quite low for these events (McGARR, 1993). Thus, for the majority of tremors induced in the deep mines of South Africa, the seismograms contain not only information related to radiated seismic energy but also data indicating the total coseismic energy release. Accordingly, these induced events can be compared in considerable detail with their laboratory counterparts. For comparison with laboratory data, the essential results for 16 mining-induced tremors are listed in Table 2. First, M_0(dev) is a scalar representing the deviatoric component of the moment tensor (McGARR, 1992b). M_0(dev) is intended to measure the shear deformation. That is,

$$M_0(\text{dev}) = \mu \sum AD \tag{12}$$

where the summation is over faults of area A and slip D and in the quartzites of the country rock $\mu = 3.76 \times 10^4$ MPa. To calculate M_0(dev), the moment tensor is first diagonalized to determine the three principal components. The deviatoric component is then obtained by subtracting the implosive component for which each entry is one third of the trace. M_0(dev), a scalar, is simply the largest absolute value of the three components of the deviatoric tensor. A double-couple tensor, for instance, has one principal component equal to zero and the other two of equal magnitude but opposite sign. Thus, for double-couple events M_0(dev) is the commonly used scalar moment M_0 (e.g., AKI, 1966; BRUNE, 1970).

Using (11) M_0(dev) is converted into a moment magnitude M. Hence, the moment magnitudes for these mining-induced tremors are meant to measure the shear deformation for comparison with laboratory events (Table 1).

Whereas in the laboratory friction experiments τ_a is measured from the difference between $\bar{\tau}$ and $\bar{\tau}_r$ (Figure 1, equation (3)), for earthquakes it is measured using (8). The radiated seismic energy E_a in (8) is estimated from

$$E(C) = 4\pi\rho C R^2 \int v^2 \, dt \tag{13}$$

where C is either the P wave speed α or the S speed β, and the integral of ground velocity squared is taken over a time window that includes the body wave pulse; ρ is density, taken as 2900 kg/m^3 here, and R is hypocentral distance. Then the total radiated energy is

$$E_a = E(\alpha) + E(\beta). \tag{14}$$

In calculating τ_a from (8), M_0(dev) is used for M_0 assuming that the implosive component of the moment tensor contributes little to the energy. This is probably a good assumption inasmuch as the implosive component contributes little to $E(\beta)$, which accounts for most of E_a.

Table 2

Data for South African mining-induced earthquakes. (Adapted from Table 1 of McGarr, 1993)

Event	Mine[a]	Depth m	M_0(dev) N-m	M	E_a J	τ_a MPa	$-\Delta V$ m^3	ΣAD m^3	$\frac{-\Delta V}{\Sigma AD}$	σ_v MPa	W J	$\bar{\tau}$ MPa	$\eta = \tau_a/\bar{\tau}$	$\bar{\tau}_r$ MPa	f_0 Hz	r_0 m	$\Delta\tau$ MPa	$\frac{\tau_a}{\Delta\tau}$	D mm
3102038	WDL	2044	3.65×10^{11}	1.7	6.39×10^5	0.066	5.0	9.7	0.52	58.1	2.91×10^8	30	0.002	29.93	14	96	0.18	0.37	0.99
3121332	WDL	2683	6.14×10^{11}	1.9	5.25×10^6	0.32	10.3	16.6	0.62	76.3	7.86×10^8	48	0.007	47.68	30	45	2.95	0.11	3.02
3141709	WDL	3081	1.50×10^{12}	2.1	2.78×10^7	0.70	−6.3	40.0	−0.16	87.7		(48)	(0.015)	47.30	18	74	1.62	0.43	7.29
3151552	WDL	2042	1.98×10^{12}	2.2	2.26×10^7	0.43	55.0	52.7	1.04	58.1	3.20×10^9	61	0.007	60.57	12	112	0.62	0.69	4.43
3151554	WDL	2205	4.85×10^{12}	2.5	6.41×10^7	0.50	74.5	129.0	0.58	62.7	4.67×10^9	36	0.014	35.50	13	103	1.94	0.26	7.04
3231839	WDL	2822	4.06×10^{12}	2.4	2.47×10^8	2.29	−10.4	107.9	−0.10	80.3		(48)	(0.048)	45.71	18	74	4.38	0.52	20.25
3241523	WDL	3243	1.75×10^{12}	2.2	3.09×10^7	0.66	29.4	47.1	0.62	92.3	2.71×10^9	58	0.011	57.34	25	54	4.86	0.14	6.52
3241529	WDL	3100	4.18×10^{12}	2.5	2.39×10^8	2.15	−12.0	111.3	−0.11	88.2		(48)	(0.045)	45.85	25[c]	54[c]	11.61	0.19	25.0
3241624	WDL	2175	5.64×10^{12}	2.5	9.15×10^7	0.61	90.0	150.0	0.60	61.9	5.57×10^9	37	0.016	36.39	16	84	4.16	0.15	8.75
3251544	WDL	2443	7.37×10^{11}	1.9	1.14×10^7	0.58	~0.0	19.6	~0.0	69.5		(48)	(0.012)	47.42	29	46	3.31	0.18	5.13
3251605	WDL	2166	2.95×10^{12}	2.3	3.31×10^7	0.36	66.0	78.0	0.84	61.6	4.07×10^9	52	0.008	51.64	15	89	1.83	0.20	5.13
0301411	HBF	2125	8.1×10^{13}	3.3	2.78×10^9	1.29	1980.0	2160.0	0.92	60.5	1.20×10^{11}	56	0.023	54.71	6	223	3.20	0.40	58.3
0301411a[b]	HBF	2055	2.75×10^{13}	3.0	7.04×10^8	0.96	426.0	731.0	0.58	58.5	2.49×10^{10}	34	0.028	33.04	8	168	2.54	0.38	23.6
0331352	HBF	2145	2.10×10^{12}	2.2	7.51×10^7	1.34	−0.7	55.9	−0.01	61.0		(48)	(0.028)	46.66	22	61	4.05	0.33	10.0
0341528	VR	2060	4.40×10^{12}	2.4	1.88×10^7	0.16	88.0	117.0	0.75	58.6	5.16×10^9	44	0.004	43.84	13	103	1.76	0.09	4.57
0271046	HBF	1918	6.19×10^{12}	2.5	1.51×10^8	0.92	150.0	165.0	0.91	54.6	8.19×10^9	50	0.018	49.08	13	103	2.48	0.37	9.0

[a] WDL: Western Deep Levels; HBF: Hartebeestfontein; VR: Vaal Reefs.

[b] Occurred less than 1 minute after event 0301411.

[c] Differs from corresponding entry, which was incorrect, in Table 1 of McGarr (1993).

As mentioned before, τ_a is a very useful source parameter in terms of relating laboratory to crustal earthquakes because of its model independence. In comparing the laboratory estimates of τ_a (Table 1) to those of the Witwatersrand tremors (Table 2) we see that in the first case $0.01 \leq \tau_a \leq 0.17$ MPa and for the latter $0.066 \leq \tau_a \leq 2.29$ MPa. There is little overlap in the two distributions.

The coseismic volume change, ΔV, which is proportional to the coseismic energy release W, is calculated from the trace of the moment tensor, denoted here $M_0(\text{vol})$, according to (AKI and RICHARDS, 1980, equation (3.34))

$$\Delta V = M_0(\text{vol})/(3\lambda + 2\mu) \tag{15}$$

where λ is one of Lamé's elastic moduli. In the deep mines under consideration here $3\lambda + 2\mu \approx 1.63 \times 10^5$ MPa. Of the 16 events listed in Table 2, the volume changes for 11 of these are negative (implosive) at a significant level. For these events the ratio $-\Delta V/\Sigma AD$ (Table 2) ranges from 0.52 to 1.04 with median and mean values of 0.62 and 0.73, respectively. The remaining five events appear to involve purely deviatoric deformation in that the ratio $-\Delta V/\Sigma AD$ is not significantly different from zero.

For the 11 events (Table 2) with convincing volume reduction, the coseismic energy release can be estimated from (e.g., COOK *et al.*, 1965)

$$W = -\sigma_v \Delta V \tag{16}$$

where σ_v (Table 2) is the ambient vertical stress due to the overburden. Equation (16) is only an approximation because the volume reduction of the stopes involves components of ground motion that are not necessarily parallel to the direction of σ_v. Because the two horizontal principal stresses in these mines tend to have at least half the magnitude of the near-vertical principal stress (e.g., MCGARR and GAY, 1978) (16) is a reasonably good estimate of the coseismic strain energy release.

From the values of W (Table 2), the average stress $\bar{\tau}$ is calculated by combining (1) and (7) to obtain

$$\bar{\tau} = \frac{\mu W}{M_0} \tag{17}$$

and we see that $\bar{\tau}$ ranges from 30 to 61 MPa, with no apparent dependence on M_0. As noted by MCGARR (1993), the median value of $\bar{\tau}$, 48 MPa, is nearly the same as a completely independent estimate of this stress based on the analysis of the energy required to produce the observed surface area of fault gouge (SPOTTISWOODE, 1980; MCGARR *et al.*, 1979) from a well-studied shear zone (ORTLEPP, 1978; GAY and ORTLEPP, 1979) in the ERPM gold mine at about 2 km depth; in that study, $\bar{\tau}$ was estimated to be about 40 MPa.

The seismic efficiencies η are then calculated from (5) and, as seen in Table 2, they are quite low. To estimate η for the five deviatoric events, the median value for $\bar{\tau}$ of 48 MPa (shown in parentheses) was assumed. The efficiencies for these

mining-induced events ranging from 0.002 to 0.048, tend to be somewhat lower than for laboratory events, most of which fall in the range 0.04 to 0.080 (Table 1). For the sake of additional comparison with the laboratory results (Table 1), $\bar{\tau}_r$, estimated from (3), is listed in Table 2 where we see that both $\bar{\tau}$ and $\bar{\tau}_r$ exceed their corresponding laboratory estimates by nearly two orders of magnitude.

The source frequencies f_0 are simply the inverse source durations measured directly from the S wave pulse widths (McGARR, 1993). Although corner frequencies are more traditionally measured from seismic spectra (BRUNE, 1970), the exceptionally clear waveforms of the 16 events listed in Table 2 (e.g., McGARR, 1992a) permitted the more direct measurement of f_0.

In contrast to the entries in Table 2 discussed to this point, which are either direct measurements or model-independent (those extending from f_0 leftward), the remaining four quantities result from model-dependent calculations. r_0, the source radius, calculated using (10) depends on Brune's model, but results from such estimates have received observational confirmation (e.g., HANKS and WYSS, 1972; McGARR, 1991). In fact, the source radii r_0 calculated here are consistent with the dimensions of the regions of the abutting rock mass over which the mining-induced stress changes are significant (e.g., McGARR *et al.*, 1975).

The stress drop $\Delta\tau$ (seismic), calculated from (11), is yet more model-dependent, incorporating the model dependence of r_0 together with the assumption that fault slip involves homogeneous stress drop across a penny-shaped crack, as mentioned before. In contrast with r_0, however, there has been no independent confirmation whatsoever regarding the actual significance of $\Delta\tau$ (seismic). Note, however, that $\Delta\tau$ (seismic) values listed in Table 2, ranging from 0.18 to 11.61 MPa fall in much the same range as those calculated for other mining-induced (e.g., SPOTTISWOODE and McGARR, 1975) as well as natural crustal earthquakes (e.g., FLETCHER *et al.*, 1984).

The ratio $\tau_a/\Delta\tau$(seismic) (Table 2) ranges from 0.09 to 0.69. Although this range is similar to that for the corresponding laboratory ratios, 0.04 to 0.45, it is probably best not to attach a great deal of significance to this agreement because in Table 2 the ratios compare τ_a, which is model-independent to $\Delta\tau$ (seismic), which is model-dependent. Taken at face value, however, these ratios indicate that for both the laboratory and the mining-induced events, overshoot occurs (Figure 1) in that nearly all of the ratios are less than 0.5.

The final entry in Table 2, fault slip D is estimated for the mine tremors using (McGARR, 1991)

$$D = 8.1R\underline{v}/\beta \tag{18}$$

where $\underline{v}$ is the peak velocity of the S wave pulse. Although (18) is a model-dependent equation, underground observations of D (McGARR, 1991) tend to confirm its validity. As seen in Table 2, D ranges from about 1 to 58 mm, whereas for the laboratory events (Table 1) the same range is 0.062 to 0.145 mm.

In terms of the primary conclusions of this report the most significant quantities listed in Table 2 are E_a and τ_a. The source of error of most concern in estimating

E_a is the effect of attenuation or limited bandwidth. All estimates of E_a are from data recorded at underground sites with source-to-site ray paths ranging from 1 to 2 km. Q for shear waves over these paths is approximately 400 (CHURCHER, 1990). Filtering experiments on the data indicate that energy in the frequency range above 50 Hz contributes almost nothing to the energy. At 50 Hz, the effect of Q on the shear wave amplitude is only a 20 percent reduction for a ray path of 2 km. Thus, it seems unlikely that either E_a or τ_a (Table 2) are reduced to any appreciable extent by the effects of either band-limited recording or attenuation during wave propagation.

Induced Earthquakes in Canada

GIBOWICZ *et al.* (1991, Table 1) presented source parameters for 155 events recorded in the Underground Research Laboratory at depths near 400 m in granite with moment magnitudes ranging from -3.6 to -1.8; thus, nearly all of these URL events are smaller than the laboratory earthquakes reviewed here (Table 1). These tiny URL events occur in granite within about 2 m of the sidewall of a vertical shaft 2.3 m in radius (TALEBI and YOUNG, 1990) where the ambient state of deviatoric stress has been amplified by a factor of approximately two due to the circular shaft (e.g., VERNIK and ZOBACK, 1989). According to MARTIN and YOUNG (1993), the maximum principal horizontal stress at depths near 400 m is 55 MPa and the minimum principal stress, vertically oriented, is about 14 MPa. If the horizontal principal stress is amplified roughly two-fold within the zone of seismicity then the typical shear stress acting to produce fault slip is of the order of 48 MPa, corresponding to $\bar{\tau}$ in (1). For comparison, values of τ_a for these URL events range from 0.016 to 2.43 MPa (GIBOWICZ *et al.*, 1991, Table 1), indicating from (5) approximate seismic efficiencies from 0.0003 to 0.051, a range that is similar to that of the Witwatersrand mine tremors (Table 2), but generally lower than the range of laboratory values (Table 1).

The other set of Canadian tremors, induced at depths near 710 m in the Strathcona mine, are of interest here because, at a given magnitude, or moment, the seismic efficiencies of these events are substantially lower than those at the URL, as will be seen. This essential difference between the URL and Strathcona earthquakes is especially persuasive because the same instrumentation and methodologies were employed in both studies (GIBOWICZ *et al.*, 1991; URBANCIC and YOUNG, 1993).

Scaling

Having reviewed the techniques used to measure seismic source processes in the laboratory (Table 1) and in deep mines (Table 2), we are now in a position to find out how these phenomena relate to each other.

Apparent Stress

First, consider apparent stress τ_a, measured using (3) for the laboratory events and (8) for the earthquakes. This commonly-estimated parameter is useful for assessing scaling effects because of its lack of model dependence. We see that the plot of τ_a (Figure 2) for some major crustal earthquakes, as well as laboratory and mining-induced events, reveals some interesting effects.

First, over nearly 18 orders of magnitude in seismic moment the apparent stress falls in the range of 0 to 10 MPa, almost without exception. Thus, globally, τ_a shows no systematic dependence on M_0, an observation that lends support to the idea that earthquakes generally are "constant stress drop" phenomena (e.g., HANKS, 1977, 1992; ABERCROMBIE and LEARY, 1993).

Second, the individual sequences (Figure 2), either mining-induced or laboratory, exhibit very strong scaling. For the laboratory events, this strong scaling ($\tau_a \sim M_0$) is anticipated because, as mentioned before, the fault area is fixed. For the mining-induced events, however, the scaling, almost as strong as that for the laboratory events, is unanticipated in view of the commonly-assumed "constant-stress-drop" hypothesis (e.g., HANKS, 1992). Using the results of the laboratory

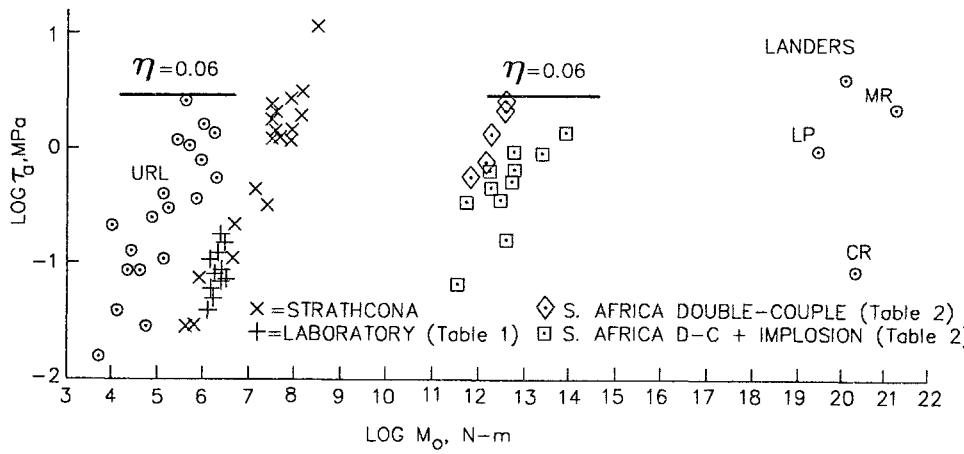

Figure 2

log τ_a as a function of log M_0 for mining-induced earthquakes, laboratory stick-slip friction events, and major crustal earthquakes. The 19 URL data plotted here were selected from 155 events listed in Table 1 of GIBOWICZ *et al.* (1991) so as to be representative of the total range of both M_0 and τ_a. Similarly, the 20 Strathcona data were selected from 85 events listed in Table 1 of URBANCIC and YOUNG (1993). The South African data are from Table 2 of this report. The symbols labeled DC represent the double-couple mechanism whereas DC + IMP is for the 11 events showing a substantial implosive component of deformation. For the earthquake data, the points labeled LP (Loma Prieta, 1989), MR (Macquarie Ridge, 1989) and CR (Costa Rica, 1983) are from HOUSTON (1990). The datum for the 1992 Landers earthquake was reported by KANAMORI *et al.* (1992) but then revised downward by KANAMORI (written communication, 1993). The horizontal lines above the URL and South African data represent $\tau_a/\bar{\tau} = 0.06$ with $\bar{\tau} = 48$ MPa.

events for guidance, it seems reasonably clear that the strong scaling of τ_a for the individual sets of mining-induced events (Figure 2) indicates a weak dependence of source dimension on M_0, a point to which I return.

Third, the data on the right-hand side of Figure 2 indicate, for natural crustal earthquakes in various tectonic settings, values of τ_a that fall in the same range as for the induced and laboratory events. Thus, at least in terms of apparent stress, these major crustal earthquakes appear to be the same phenomena as even the tiniest induced events.

Maximum Fault Slip

Over about 14 orders of magnitude in seismic moment, maximum fault slip D appears in general to scale approximately as $M_0^{1/3}$ (Figure 3) as it should, to the extent that D is proportional to source dimension (e.g., equation (7)). On the left-hand side of Figure 3 the laboratory measurements of D (Table 1) scale as M_0, as explained before, and in the middle portion of the figure, D, from Table 2, inferred using (18) shows scaling much stronger than $M_0^{1/3}$. The point at $M_0 \approx 5 \times 10^{15}$ N-m corresponds to a mining-induced tremor for which the maximum fault slip was measured *in situ* (BRUMMER and RORKE, 1990; MCGARR, 1991). The two data on the right-hand side of Figure 2 are for two recent

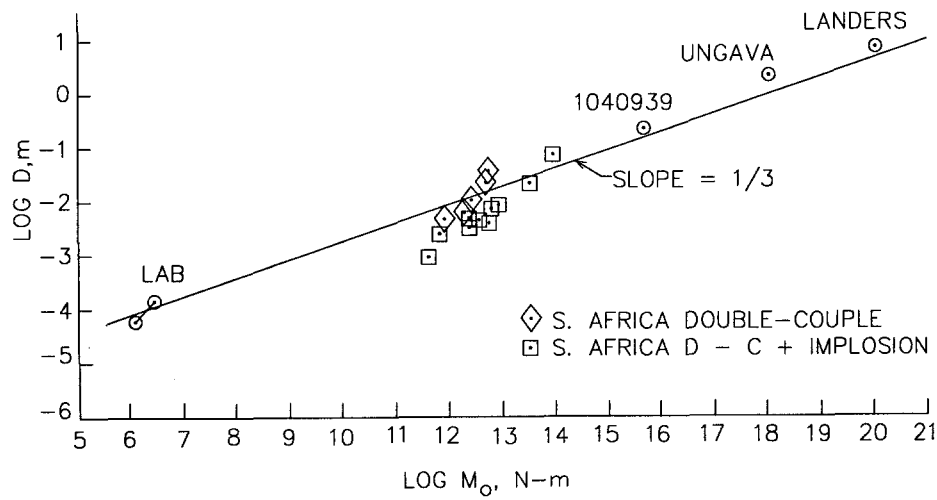

Figure 3

log D as a function of log M_0 for laboratory events, mining-induced tremors and two earthquakes. For the laboratory stick-slip events only the two extreme data are shown; all of the other laboratory data (Table 1) fall on the line joining these two extreme points. The point labeled 1040939 was reported by MCGARR (1991). For this event, the fault slip D was measured *in situ* by BRUMMER and RORKE (1990). The line representing $D \propto M_0^{1/3}$ was drawn to pass through the laboratory data. The point labeled Ungava is from ADAMS *et al.* (1991) and the Landers datum was reported by SIEH *et al.* (1993).

earthquakes that produced remarkably well-defined surface slip (ADAMS *et al.*, 1991; SIEH *et al.*, 1993).

Thus, as for apparent stress, simple scaling principles ($D \sim M_0^{1/3}$) seem sufficient for globally relating slip measured in the laboratory upward to that for the mining-induced tremors and then to slip associated with the yet larger crustal earthquakes. Accordingly, in $D-M_0$ space the laboratory stick-slip events appear to be the same phenomena as earthquakes, induced or natural. Note, however, that both the laboratory and mining-induced events show individual scaling much stronger than $D \sim M_0^{1/3}$.

Discussion

To this point I have reviewed a body of evidence that tends to confirm the suggestion (BRACE and BYERLEE, 1966) that stick-slip friction in the laboratory is indeed the same essential phenomenon as crustal earthquakes. The more interesting question, so far avoided here, is whether or not the friction experiments provide useful insights in interpreting crustal earthquake data.

Consider, for example, the proposal by SCHOLZ (1990, p. 91) that, based on laboratory evidence, the stress drop (Figure 1) tends to be of the order of 10 percent of the total shear stress acting on the fault. If this, or some version of this, is so, then seismologists would have the capability of using seismic data to estimate absolute levels of deviatoric stress in the seismogenic crust.

To pursue this exciting possibility, consider first how the stress changes in the laboratory experiments (Table 1) relate to the average stresses $\bar{\tau}$ acting on the fault. We see that one measure of stress change, τ_a, tends to be close to its median value of 0.06 of $\bar{\tau}$, as noted before by LOCKNER and OKUBO (1983), with the ratio $\tau_a/\bar{\tau}$ ranging from 0.012 to 0.08 (Table 1). This ratio appears to be independent of either M_0 or $\bar{\tau}$.

Similar remarks apply to the stress drops $\Delta\tau$ measured in the laboratory in that $\Delta\tau/\bar{\tau}$ ranges from 0.12 to 0.30, with a median value of 0.23. Again, there appears to be no systematic dependence of this ratio on either $\bar{\tau}$ or M_0.

To summarize the laboratory evidence (Table 1)

$$\tau_a/\bar{\tau} \simeq 0.06 \tag{19}$$

and

$$\Delta\tau/\bar{\tau} \simeq 0.23. \tag{20}$$

Each of these ratios appears to be independent of both M_0 and confining pressure σ_n at least over the range included in Table 1.

A comparison of the behavior of $\bar{\tau}$ in the laboratory experiments and in the South African gold mines provides the first indication of complications in general-

izing the laboratory results, (19) and (20), to crustal earthquakes. Whereas for the laboratory data, $\bar{\tau}$ (Figure 4) scales with M_0 in the same way as τ_a (Figure 2), $\bar{\tau}$ for the mining-induced events is independent of M_0 in contrast to τ_a which, as noted before, scales strongly with M_0. Similarly, the ratio $\tau_a/\bar{\tau}$ $(=\eta)$ shows a much broader variation in the mines (Table 2) than in the laboratory (Table 1), in a lower range with little overlap.

The behavior of $\Delta\tau/\bar{\tau}$ for mining-induced events (Table 2) is also quite different from that of the laboratory events (Table 1), again showing a broader range. In contrast to the laboratory results, (20), the median of $\Delta\tau/\bar{\tau}$ for the mine tremors (Table 2) is only 0.065.

As there is no reason to suspect that the physics of fault slip in the deep gold mines differs in any essential way from that in the laboratory, it seems most likely that the behavioral differences in $\tau_a/\bar{\tau}$ and $\Delta\tau/\bar{\tau}$ are a consequence of contrasts in fault slip configuration. Whereas for the laboratory stick-slip events (Table 1) the slip D is homogeneous over a planar surface of area 0.8 m^2, there is abundant evidence to the effect that for the mine tremors the slip is quite inhomogeneous (e.g., SPOTTISWOODE and MCGARR, 1975; MCGARR *et al.*, 1975). In particular, within the idealized penny-shaped source of radius r_0 there are almost certainly regions where slip is much greater than average (asperities) and those for which slip is zero ("barriers" in the terminology of DAS and AKI, 1977).

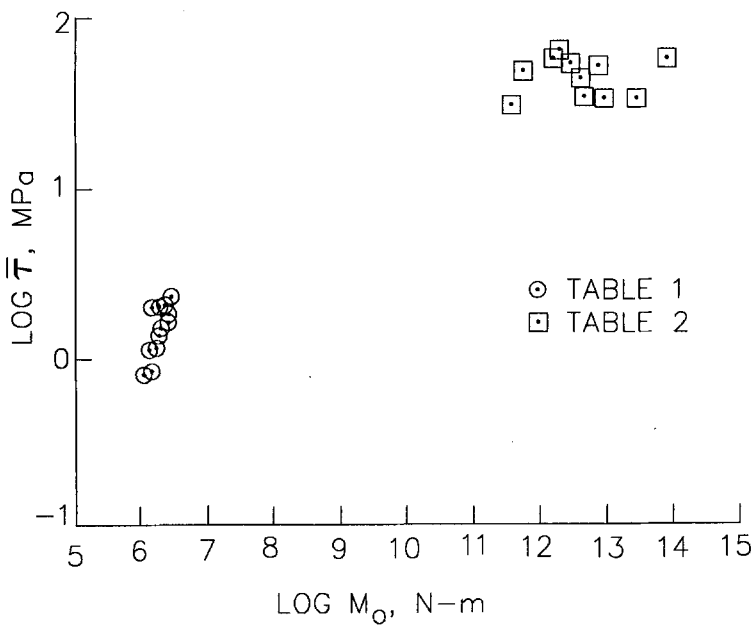

Figure 4
log $\bar{\tau}$ as a function of log M_0. These data are from Tables 1 and 2.

Thus, the working hypothesis proposed here entails a seismic source model for which, in a given sequence of earthquakes, neither the source dimension nor the average applied stress causing slip varies significantly. Instead, the primary variability involves the distribution of barriers to slip within the source radius.

The seismic source model entailing the failure of an asperity, developed by DAS and KOSTROV (1983) and MCGARR (1991), is especially convenient for illustrating the effect of barriers on the apparent stress. An asperity of radius r_0 that fails due to an applied stress $\bar{\tau}$ will experience maximal homogeneous slip D if there are no barriers within the asperity. With increasing barrier area, the average slip $\bar{D}$ decreases. Thus,

$$\bar{D} \leq D. \tag{21}$$

To calculate the apparent stress, (8) needs to be evaluated, which in turn, involves E_a and M_0. From (7)

$$M_0 = \mu \pi r_0^2 \bar{D} \tag{22}$$

and from (13) and (14)

$$E_a \approx 4\pi\rho\beta R^2 \int_0^T v^2 \, dt \tag{23}$$

where T is the duration of the S-wave pulse and, for the present purpose, the small contribution of the P wave to the total radiated energy is neglected. From equation (11) of MCGARR (1991, with $k = 2.34$), (23) is readily evaluated for the S-wave pulse to yield

$$E_a \approx 0.61 \mu \bar{D}^2 r_0. \tag{24}$$

Then combining (8), (22) and (24) gives for the apparent stress

$$\tau_a = 0.19 \mu \bar{D} / r_0. \tag{25}$$

It is important to note that any plausible seismic source model (e.g., BRUNE, 1970; MADARIAGA, 1976; BOATWRIGHT, 1980) would yield the same functional form for τ_a as (25). Thus, the dependence of τ_a on $\bar{D}/r_0$ is not specific to the source model used here (MCGARR, 1991).

The main point, then, is that, even though fault slip over an asperity may be physically identical to that in laboratory experiments, the presence of barriers reduces $\bar{D}$ and, therefore, τ_a, assuming fixed r_0 in (25). Accordingly, for an asperity without internal barriers, both M_0 and E_a are maximal, with $\bar{D} = D$ and τ_a complies with (19). Hence, (19) represents, I think, the upper bound result for the earthquake sequences considered here.

As seen in Figure (2), (19) does, indeed, seem to be a reasonable upper bound for the two earthquake sequences for which estimates of $\bar{\tau}$ are available. For both

the South African and Canadian URL events $\bar{\tau} \simeq 48$ MPa and so from (19), (21) and (25), $\tau_a \leq 2.9$ MPa. This inequality is clearly in accord with the data.

Assuming that (19) applies to other earthquake sequences as well, one can use reliable observations of apparent stress to estimate observational upper bounds, which then yield $\bar{\tau}$, the absolute level of deviatoric stress acting to produce seismic slip. Thus, although individual values of τ_a cannot be related directly to the ambient deviatoric stress, suites of τ_a estimates can yield upper bounds that in turn may be related to $\bar{\tau}$ according to (19). Alternatively, individual values of τ_a may yield lower bound estimates of $\bar{\tau}$. For instance, the estimate of $\tau_a \simeq 4.1$ MPa for the Landers earthquake (Figure 2) corresponds to an average loading stress $\bar{\tau}$ of 65 to 70 MPa, if (19) is appropriate for crustal earthquakes.

One could, in principle, analyze seismic stress drops $\Delta\tau$ in the same way just done for τ_a but the model dependence of the estimates of $\Delta\tau$ for earthquakes presents an essential problem. As mentioned before, it is not clear exactly how these model-dependent estimates of $\Delta\tau$ for earthquakes relate to the directly-measured laboratory values (Figure 1). For what it's worth, however, let us suppose that $\Delta\tau$ for earthquakes can be realistically compared to laboratory values. Then, using the same argument as before for τ_a, (20) represents an upper bound for $\Delta\tau$ for any particular sequence. For both the URL (GIBOWICZ *et al.*, 1991) and the South African events, with $\bar{\tau} = 48$ MPa, $\Delta\tau \leq 11$ MPa. As seen in Table 2, all but one of the South African tremors adheres to this bound, with event 325 1539 exceeding the limit by an insignificant margin. For the URL events the values of $\Delta\tau$ listed in Table 1 of GIBOWICZ *et al.* (1991) conform to $\Delta\tau \leq 3.1$ MPa, and, thus, are compatible with an upper bound of 11 MPa.

Concluding Remarks

The evidence reviewed here indicates that laboratory stick-slip friction experiments can provide some very useful insights regarding the mechanics of induced earthquakes and, presumably, natural crustal earthquakes as well. Because the physical processes of the laboratory and induced events appear to be identical there is considerable benefit, as demonstrated here, to be derived by relating earthquake source parameters, measured from seismograms, to their counterparts in the laboratory experiments. In this way, the laboratory results can be used to resolve many longstanding questions regarding earthquake source processes including the three posed just after equation (8) in the Introduction.

First, the behavior of apparent stress τ_a (Figure 2) for individual sequences of both induced and laboratory earthquakes does not conform to the normally-expected "constant stress-drop" scaling (e.g., HANKS, 1977) for which τ_a would show no systematic dependence on seismic moment. Instead, for each data set, τ_a shows quite a strong and systematic dependence on M_0. This strong scaling is easy to

understand in the case of the laboratory events because the fault area is fixed at 0.8 m^2 which means that $\tau_a \propto D/r_0 \propto M_0$, inasmuch as the fault radius r_0 is invariant. It was somewhat surprising, however, that the scaling of the induced earthquakes (Figure 2) is much more similar to that of the laboratory events than to the constant-stress-drop expectation, for which $D \propto r_0$. It appears that the seismic source zones tend to be roughly the same size as the region over which the deviatoric stress has been substantially augmented to produce earthquakes. For the URL events, the source radii r_0 (Table 1 of GIBOWICZ *et al.*, 1991) range from 0.24 to 0.91 m and show only a weak, poorly-defined dependence on M_0. The source dimensions ($\sim 2r_0$) of these tremors fit within the zone 1 to 2 m thick around the URL shaft (MARTIN and YOUNG, 1993) within which the deviatoric stress has been augmented by a factor of approximately two. For the South African mine tremors (Figure 2, Table 2) the corresponding dimension is about 200 m (e.g. MCGARR *et al.*, 1975).

The Strathcona events (Figure 2), whose magnitude range overlaps that of the URL tremors, helps to illustrate the effect of source dimension on τ_a. Source radii measured by URBANCIC and YOUNG (1993) ranged from 0.86 to 2.75 m, and, thus, are typically three times as large as their URL counterparts. As seen in Figure 2, in the region of moment overlap for these two sequences, τ_a for the Strathcona events is roughly a factor of 20 to 40 less than that for the URL. Combining equations (22) and (25) yields the result that $\tau_a \sim M_0/r_0^3$. Thus, for fixed M_0, we anticipate that if the source radii at Strathcona are three times as large as those of the URL, the corresponding seismic efficiencies should be about 27 times smaller, consistent with what is observed in Figure 2.

The comparison between the URL and Strathcona events raises the question of why the laboratory data tend to coincide with the Strathcona instead of the URL data in view of the close agreement between the source dimensions of the laboratory (2 m × 0.4 m) and URL ($0.48 \leq 2r_0 \leq 1.82$ m). If the mechanics of the laboratory events were identical to those of the induced earthquakes, then one would expect the laboratory measurements of τ_a to agree closely with those of the URL events, for fixed M_0.

In terms of source time history, however, the laboratory events are much more similar to the Strathcona events in that with a typical source duration (DIETERICH, 1981; LOCKNER and OKUBO, 1987) of 2.5 ms, the corresponding corner frequency of about 400 Hz yields an equivalent seismic source radius, using (10), of 2.8 m, where β is assumed to be 3000 m/s. This equivalent seismic source radius is at the top of the Strathcona range (0.86 to 2.75 m), but, far above the URL range (0.24 to 0.91 m). Thus, in terms of source time history, the "size" of the laboratory events coincides with the larger Strathcona tremors but not those of the URL. This is almost certainly the proper comparison because our estimates of the earthquake sizes rely completely on the source time histories.

Although, for individual sequences (e.g., the URL tremors) the principal difference between large and small events involves average slip, but not source dimension, it is important to emphasize that in a global sense, the data reviewed here support the constant-stress-drop idea in that, taken together, the data of Figure 2 show no systematic variation with M_0 over an enormous range. Thus, nothing presented here should be construed as evidence contrary to what was presented by HANKS (1977), for example, who considered a very global data set.

Second, with regard to the efficiency of earthquakes ($\eta = \tau_a/\bar{\tau}$) the results reviewed here (e.g., Table 2) indicate efficiencies that are even lower than those of the laboratory stick-slip events, for which $\eta \simeq 0.06$ seems to be typical. For both the URL and the South African induced earthquake data sets $\eta < 0.06$.

A related issue involves the behavior of the dynamic coefficient of friction, or resisting stress τ_r, as a function of fault slip. In the laboratory stick-slip experiments, as exemplified in Figure 1, τ_r diminishes, at the initiation of slip, from its static to an average dynamic value about which it fluctuates closely for the duration of the event. Although much more exotic behavior of τ_r has been postulated for earthquakes (e.g., HEATON, 1990) involving a very drastic reduction in τ_r followed by "healing" or increase in the final stages of the event (an "undershoot" scenario) the small ratios $\tau_a/\bar{\tau}$ observed for the induced tremors do not provide appreciable scope for such effects; instead it seems almost certain that τ_r for these induced events (e.g., Table 2) behaves in much the same way as seen in Figure 1.

Third, and perhaps most interestingly, although the ratios $\tau_a/\bar{\tau}$ for laboratory and mining-induced events are similarly quite small, in more detail they show profound differences. Whereas, for the laboratory events $\tau_a/\bar{\tau}$ shows little variation about 0.06, the same ratio for the induced events increases systematically with M_0 such that 0.06 appears to be an upper bound. This observed contrast in behavior motivates the working hypothesis that for mining-induced events, and possibly natural crustal earthquakes as well,

$$\tau_a/\bar{\tau} \leq 0.06 \tag{26}$$

with equality corresponding to homogeneous slip over the entire fault plane, as is the case in the laboratory. For all other events, the inequality is a consequence of barriers to slip within the source zone that reduce the average slip.

This hypothesis, although quite exciting in that it provides an important link between seismic data and the hypocentral environment (e.g., MCGARR, 1984; SCHOLZ, 1990), is nonetheless tentative. Needless to say, much additional research, both in the laboratory and involving induced earthquakes, is necessary to test the generality of (26). Possibly differences in the experimental configuration, differences in fault zone material, or the presence of fluids would yield substantially different results in the laboratory. In the field, it is clearly necessary to study additional earthquake sequences for which $\bar{\tau}$ can be estimated.

Acknowledgments

I thank T. Hanks and J. Dieterich for insightful reviews of this manuscript and C. Sullivan for valuable editorial assistance. I am grateful to D. Martin, T. Urbancic, and R. Abercrombie for some useful suggestions and to H. Kanamori for providing the revised energy estimate for the 1992 Landers earthquake. M. Blanpied and C. Marone helped considerably to motivate this analysis by organizing the Special Issue.

REFERENCES

ABERCROMBIE, R., and LEARY, P. (1993), *Source Parameters of Small Earthquakes Recorded at 2.5 km Depth, Cajon Pass, Southern California: Implications for Earthquake Scaling*, Geophys. Res. Lett. *20*, 1511–1514.

ADAMS, J., WETMILLER, R. J., HASEGAWA, H. S., and DRYSDALE, J. (1991), *The First Surface Faulting from a Historical Intraplate Earthquake in North America*, Nature *352*, 617–619.

AKI, K. (1966), *Generation and Propagation of G Waves from the Niigata Earthquake of June 16, 1964, 2, Estimation of Earthquake Moment, Released Energy, and Stress-strain Drop from the G Wave Spectrum*, Bull. Earthquake Res. Inst. Tokyo Univ. *44*, 73–88.

AKI, K., and RICHARDS, P. G., *Quantitative Seismology: Theory and Methods* (Freeman, Cooper, San Francisco, CA 1980).

BOATWRIGHT, J. (1980), *A Spectral Theory for Circular Seismic Sources; Simple Estimates of Source Dimension, Dynamic Stress Drop, and Radiated Seismic Energy*, Bull. Seismol. Soc. Am. *70*, 1–27.

BRACE, W. F., and BYERLEE, J. D. (1966), *Stick Slip as a Mechanism for Earthquakes*, Science *153*, 990–992.

BRUMMER, R. K., and RORKE, A. J., *Case studies on large rockbursts in South African gold mines.* In *Rockbursts and Seismicity in Mines* (ed. Fairhurst, C.) (Balkema, Rotterdam 1990) pp. 323–329.

BRUNE, J. N. (1970), *Tectonic Stress and the Spectra of Seismic Shear Waves from Earthquakes*, J. Geophys. Res. *75*, 4997–5009. (Correction (1971), J. Geophys. Res. *76*, 5002.)

BRUNE, J. N., *The physics of earthquake strong motion.* In *Seismic Risk and Engineering Decisions* (ed. Lomnitz, C., and Rosenbluth, E.) (Elsevier, New York 1976) pp. 141–177.

CHURCHER, J. M., *The effect of propagation path on the measurement of seismic parameters.* In *Rockbursts and Seismicity in Mines* (ed. Fairhurst, C.) (Balkema, Rotterdam 1990) pp. 205–209.

COOK, N. G. W., *The seismic location of rockbursts.* In *Proc Fifth Rock Mechanics Symposium* (Pergamon Press, Oxford 1963) pp. 493–516.

COOK, N. G. W., HOEK, E., PRETORIUS, J. P. G., ORTLEPP, W. D., and SALAMON, M. D. G. (1965), *Rock Mechanics Applied to the Study of Rockbursts*, J. S. Afr. Inst. Min. Metall. *66*, 435–528.

DAS, S., and AKI, K. (1977), *Fault Plane with Barriers: A Versatile Earthquake Model*, J. Geophys. Res. *82*, 5658–5670.

DAS, S., and KOSTROV, B. V. (1983), *Breaking of a Single Asperity: Rupture Process and Seismic Radiation*, J. Geophys. Res. *88*, 4277–4288.

DIETERICH, J. H. (1979), *Modelling of Rock Friction, 1. Experimental Results and Constitutive Equations*, J. Geophys. Res. *84*, 2161–2168.

DIETERICH, J. H. (1981), *Potential for Geophysical Experiments in Large-scale Tests*, Geophys. Res. Lett. *8*, 653–656.

DIETERICH, J. H. (1992), *Earthquake Nucleation on Faults with Rate- and State-dependent Strength*, Tectonophysics *211*, 115–134.

FLETCHER, J. B., BOATWRIGHT, J., HAAR, L., HANKS, T., and MCGARR, A. (1984), *Source Parameters for Aftershocks of the Oroville, California, Earthquake*, Bull. Seismol. Soc. Am. *74*, 1101–1123.

GAY, N. C., and ORTLEPP, W. D. (1979), *Anatomy of a Mining-induced Fault Zone*, Geol. Soc. Am. Bull. *90*, 47–58.

GIBOWICZ, S. J., YOUNG, R. P., TALEBI, S., and RAWLENCE, D. J. (1991), *Source Parameters of Microseismic Events at the Underground Research Laboratory in Manitoba, Canada: Scaling Relations for the Events with Moment Magnitude Smaller than −2*, Bull. Seismol. Soc. Am. *81*, 1157–1182.

HANKS, T. C. (1977), *Earthquake Stress Drops, Ambient Tectonic Stress and Stresses that Drive Plate Motions*, Pure. Appl. Geophys. *115*, 441–458.

HANKS, T. C. (1992), *Small Earthquakes, Tectonic Forces*, Science *256*, 1430–1432.

HANKS, T. C., and WYSS, M. (1972), *The Use of Body Wave Spectra in the Determination of Seismic Source Parameters*, Bull. Seismol. Soc. Am. *62*, 561–589.

HANKS, T. C., and KANAMORI, H. (1979), *A Moment Magnitude Scale*, J. Geophys. Res. *84*, 2348–2350.

HEATON, T. H. (1990), *Evidence for, and Implications of Self-healing Pulse of Slip in Earthquake Rupture*, Phys. Earth Planet. Sci. *16*, 1–20.

HOUSTON, H. (1990), *A Comparison of Broadband Source Spectra, Seismic Energies, and Stress Drops of the 1989 Loma Prieta and 1988 Armenian Earthquakes*, Geophys. Res. Lett. *17*, 1413–1416.

KANAMORI, H., HONG-KIE, T., DREGER, D., and HAUKSSON, E. (1992), *Initial Investigation of the Landers, California, Earthquake of 28 June 1992 Using Terrascope*, Geophys. Res. Lett. *19*, 2267–2270.

KEILIS-BOROK, V. I. (1959), *On Estimation of the Displacement in an Earthquake Source and of Source Dimension*, Ann. Geofis. *12*, 205–214.

LACHENBRUCH, A. H., and MCGARR, A. (1990), *Stress and heat flow*. U.S. Geological Survey Professional Paper *1515*, *The San Andreas Fault System* (ed. Wallace, R.) pp. 261–277.

LOCKNER, D. A., and OKUBO, P. G. (1983), *Measurements of Frictional Heating in Granite*, J. Geophys. Res. *88*, 4313–4320.

MADARIAGA, R. (1976), *Dynamics of an Expanding Circular Fault*, Bull. Seismol. Soc. Am. *66*, 639–666.

MARTIN, C. D., and YOUNG, R. P., *The effect of excavation-induced seismicity on the strength of Lac du Bonnet granite*. In *Rockbursts and Seismicity in Mines* (ed. Young, R. P.) (Balkema, Rotterdam 1993) pp. 367–371.

MCGARR, A. (1976), *Seismic Moments and Volume Changes*, J. Geophys. Res. *81*, 1487–1494.

MCGARR, A. (1984), *Scaling of Ground Motion Parameters, State of Stress, and Focal Depth*, J. Geophys. Res. *89*, 6969–6979.

MCGARR, A. (1991), *Observations Constraining Near-source Ground Motion Estimated from Locally Recorded Seismograms*, J. Geophys. Res. *96*, 16,495–16,508.

MCGARR, A. (1992a), *An Implosive Component in the Seismic Moment Tensor of a Mining-induced Tremor*, Geophys. Res. Lett. *19*, 1579–1582.

MCGARR, A. (1992b), *Moment Tensors of Ten Witwatersrand Mine Tremors*, Pure Appl. Geophys. *139*, 781–800.

MCGARR, A., *Factors influencing the strong ground motion from mining-induced tremors*. In *Rockbursts and Seismicity in Mines* (ed. Young, R. P.) (Balkema, Rotterdam 1993) pp. 3–12.

MCGARR, A., SPOTTISWOODE, S. M., and GAY, N. C. (1975), *Relationship of Mine Tremors to Induced Stresses and to Rock Properties in the Focal Region*, Bull. Seismol. Soc. Am. *65*, 981–993.

MCGARR, A., and GAY, N. C. (1978), *State of Stress in the Earth's Crust*, Ann. Rev. Earth Planet. Sci. *6*, 405–436.

MCGARR, A., SPOTTISWOODE, S. M., GAY, N. C., and ORTLEPP, W. D. (1979), *Observations Relevant to Seismic Driving Stress, Stress Drop, and Efficiency*, J. Geophys. Res. *84*, 2251–2261.

MCGARR, A., BICKNELL, J., SEMBERA, E., and GREEN, R. W. E. (1989), *Analysis of Exceptionally Large Tremors in Two Gold Mining Districts of South Africa*, Pure Appl. Geophys. *129*, 295–307.

ORTLEPP, W. D. (1978), *The Mechanism of a Rockburst*, Proc. of the 19th U.S. Rock Mechanics Symposium, University of Nevada, Reno, 476–483.

SAVAGE, J. C., and WOOD, M. D. (1971), *The Relationship Between Apparent Stress and Stress Drop*, Bull. Seismol. Soc. Am. *61*, 1381–1388.

SCHOLZ, C. H., *The Mechanics of Earthquakes and Faulting* (Cambridge Univ. Press, Cambridge, U.K. 1990).

SIEH, K. E. *et al.* (1993), *Near-field Investigations of the Landers Earthquake Sequence, April to July 1992*, Science *260*, 171–176.

SPOTTISWOODE, S. M. (1980), *Source Mechanism Studies on Witwatersrand Seismic Events*, Ph.D. Thesis, University of Witwatersrand, Johannesburg, South Africa.

SPOTTISWOODE, S. M., and MCGARR, A. (1975), *Source Parameters of Tremors in a Deep-level Gold Mine*, Bull. Seismol. Soc. Am. *65*, 93–112.

TALEBI, S., and YOUNG, R. P., *Failure mechanism of crack propagations induced by shaft excavation at the Underground Research Laboratory*. In *Rock at Greath Depth 3* (eds. Maury, V., and Fourmaintraux, D.) (Balkema, Rotterdam 1990) pp. 1455–1461.

URBANCIC, T. I., and YOUNG, R. P. (1993), *Space-time Variations in Source Parameters of Mining-induced Seismic Events with $M < 0$*, Bull. Seismol. Soc. Am. *83*, 378–397.

VASSILIOU, M. S., and KANAMORI, H. (1982), *The Energy Release in Earthquakes*, Bull. Seismol. Soc. Am. *72*, 371–387.

VERNIK, L., and ZOBACK, M. D., *Effects of rock elastic and strength properties in estimation of the state of stress at depth*. In *Rock at Greath Depth 2* (eds. Maury, V., and Fourmaintraux, D.) (Balkema, Rotterdam 1990) pp. 1033–1040.

WALSH, J. B. (1971), *Stiffness in Faulting and Friction Experiments*, J. Geophys. Res. *76*, 8597–8598.

WYSS, M., and BRUNE, J. N. (1968), *Seismic Moment, Stress, and Source Dimensions for Earthquakes in the California-Nevada Region*, J. Geophys. Res. *73*, 4681–4694.

YOUNG, R. P., TALEBI, S., HUTCHINS, D. A., and URBANCIC, T. I. (1989), *Analysis of Mining-induced Microseismic Events at Strathcona Mine, Sudbury, Canada*, Pure Appl. Geophys. *129*, 455–474.

(Received October 6, 1993, revised January 26, 1994, accepted February 2, 1994)